

## Physiochemical Pathway for Cyclic Dehydrogenation and Rehydrogenation of LiAlH<sub>4</sub>

Jun Wang, Armin D. Ebner, and James A. Ritter\*

Contribution from the Department of Chemical Engineering, Swearingen Engineering Center, University of South Carolina, Columbia, South Carolina 29208

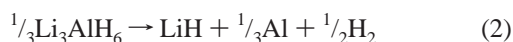
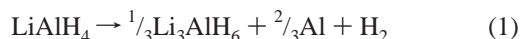
Received January 3, 2006; E-mail: ritter@enr.sc.edu

**Abstract:** A five-step physiochemical pathway for the cyclic dehydrogenation and rehydrogenation of LiAlH<sub>4</sub> from Li<sub>3</sub>AlH<sub>6</sub>, LiH, and Al was developed. The LiAlH<sub>4</sub> produced by this physiochemical route exhibited excellent dehydrogenation kinetics in the 80–100 °C range, providing about 4 wt % hydrogen. The decomposed LiAlH<sub>4</sub> was also fully rehydrogenated through the physiochemical pathway using tetrahydrofuran (THF). The enthalpy change associated with the formation of a LiAlH<sub>4</sub>·4THF adduct in THF played the essential role in fostering this rehydrogenation from the Li<sub>3</sub>AlH<sub>6</sub>, LiH, and Al dehydrogenation products. The kinetics of rehydrogenation was also significantly improved by adding Ti as a catalyst and by mechanochemical treatment, with the decomposition products readily converting into LiAlH<sub>4</sub> at ambient temperature and pressures of 4.5–97.5 bar.

### Introduction

Implementation of a hydrogen economy presents a significant challenge, with hydrogen storage being one of the biggest, potentially show stopping, roadblocks.<sup>1</sup> Many hydrogen storage methods have been proposed;<sup>1–6</sup> however, despite all of the intense research efforts, the Department of Energy's goals of 6.5 wt % H<sub>2</sub> (system basis) and 62 kg H<sub>2</sub>/m<sup>3</sup> have not been met. In recent studies, metal complex hydrides, due to their high hydrogen storage capacity, have been exhibiting the potential to meet these storage requirements.<sup>7–11</sup>

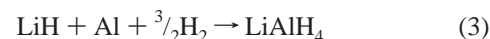
LiAlH<sub>4</sub>, which can release up to 7.9 wt % hydrogen according to the following reactions:



has exhibited very impressive dehydrogenation kinetics at reasonable temperatures.<sup>10–12</sup> Still, the reversible storage of

hydrogen in LiAlH<sub>4</sub> has not been conclusively demonstrated. Although partial reversibility of the second reaction in eq 2 has been claimed,<sup>11</sup> recent results have shown no reversibility of either reaction in eqs 1 and 2 under similar conditions.<sup>12</sup>

Therefore, the main objective here is to report on the notion of using a liquid complexing agent, such as tetrahydrofuran (THF), in conjunction with a Ti catalyst and a hydrogen atmosphere during high-pressure ball milling, to promote rehydrogenation of LiAlH<sub>4</sub> from Li<sub>3</sub>AlH<sub>6</sub>, LiH, and Al through a five-step physiochemical pathway. It is shown that the THF forms a LiAlH<sub>4</sub>·4THF adduct during the rehydrogenation step according to



and possibly the reverse reaction in eq 1. It is further shown that the free energy change associated with the formation of the LiAlH<sub>4</sub>·4THF adduct in THF plays the essential role in rehydrogenation, causing it to regenerate at ambient temperature and low pressures of 4.5–97.5 bar. Finally, it is revealed that the rehydrogenation kinetics is dramatically improved by adding Ti as a catalyst and by mechanochemical treatment.

Although the direct synthesis of LiAlH<sub>4</sub> from LiH and Al in tetrahydrofuran (THF), as shown in eq 3, has been reported,<sup>13,14</sup> either little information was given or the reaction conditions and conversion were significantly different from those reported here. For example, Clasen<sup>13</sup> showed that the reaction in eq 3 occurs at 35 °C and 30 bar in a THF or diglyme solution, while no reaction occurs in diethyl ether (Et<sub>2</sub>O); however, very few details about the reaction were given. On the other hand, Ashby et al.<sup>14</sup> reported that the reaction in eq 3 occurs at 120 °C and

- Ritter, J. A.; Ebner, A. D.; Wang, J.; Zidan, R. *Mater. Today* **2003**, *9*, 18–23.
- Schlapbach, L.; Züttel, A. *Nature* **2001**, *414*, 353–358.
- Dillon, A. C.; Jones, K. M.; Bekkedahl, T. A.; Kiang, C. H.; Bethune, D. S.; Heben, M. J. *Nature* **1997**, *386*, 377–379.
- Chen, P.; Xiong, Z.; Luo, J.; Lin, J.; Tan, K. L. *Nature* **2002**, *420*, 302–304.
- Florusse, L. J.; Peters, C. J.; Schoonman, J.; Hester, K. C.; Koh, C. A.; Dec, S. F.; Marsh, K. N.; Sloan, E. D. *Science* **2004**, *306*, 469–471.
- Rosi, N. L.; Eckert, J.; Eddaoudi, M.; Vodak, D. T.; Kim, J.; O'Keefe, M.; Yaghi, O. M. *Science* **2003**, *300*, 1127–1129.
- Bogdanovic, B.; Schwickardi, M. *J. Alloys Compd.* **1997**, *253*, 1–9.
- Schüth, F.; Bogdanovic, B.; Felderhoff, M. *Chem. Commun.* **2003**, *20*, 2249–2258.
- Wang, J.; Ebner, A. D.; Prozorov, T.; Zidan, R.; Ritter, J. A. *J. Alloys Compd.* **2005**, *395*, 252–262.
- Balema, V.; Pecharsky, V.; Dennis, K. *J. Alloys Compd.* **2000**, *313*, 69–74.
- Chen, J.; Kuriyama, N.; Xu, Q.; Takeshita, H. T.; Sakai, T. *J. Phys. Chem. B* **2001**, *105*, 11214–11220.
- Wang, J.; Ebner, A. D.; Ritter, J. A. *Adsorption* **2005**, *11*, 811–816.

(13) Clasen, H. *Angew. Chem.* **1961**, *73*, 322–331.

(14) Ashby, E. C.; Brendel, G. J.; Redman, H. E. *Inorg. Chem.* **1963**, *2*, 499–504.

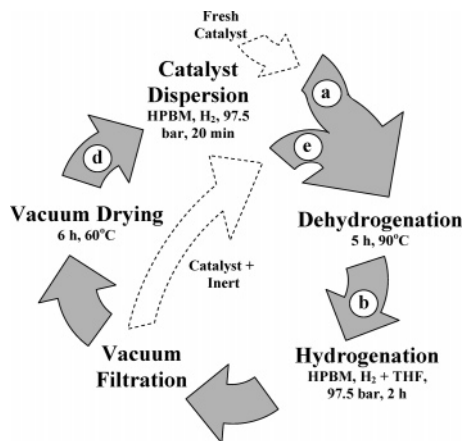


**Figure 1.** Schematic representation of the five-step physiochemical pathway for the cyclic dehydrogenation and rehydrogenation of  $\text{LiAlH}_4$ . The cycle steps consist of catalyst dispersion, dehydrogenation, rehydrogenation, vacuum filtration, and vacuum-drying. The conditions listed are not exclusive and correspond to the typical results presented in Figure 2 that were obtained for one complete cycle. The letters in the arrows correspond to the curves in Figure 2.

345 bar in THF or diglyme solution with very high conversion (>95%), while this reaction exhibits little conversion in  $\text{Et}_2\text{O}$ . However, these conditions were significantly different from those reported here for the reaction in eq 3 to proceed. Moreover, neither study even fathomed the possibility of using  $\text{LiAlH}_4$  as a hydrogen storage material.

## Results and Discussion

**Physiochemical Pathway.** The five-step physiochemical pathway is shown schematically in Figure 1. The cycle steps consist of catalyst dispersion, dehydrogenation, rehydrogenation, vacuum filtration, vacuum-drying, and then catalyst redispersion. This last step begins the first step of the second cycle and so on. Note that fresh catalyst or preferably catalyst recovered from the filtration step as insoluble residue may be used. The THF can also be easily recovered and reused. At very high conversions, this cycle represents a closed loop requiring only energy input for the cyclic dehydrogenation and rehydrogenation of  $\text{LiAlH}_4$ , a potential hydrogen storage material.

To demonstrate and explain these key steps, one characteristic dehydrogenation/rehydrogenation cycle is shown in Figure 2. These results were obtained from a 0.5 mol % Ti-doped  $\text{LiAlH}_4$  sample investigated by thermogravimetric analysis. First, the 0.5 mol % Ti-doped  $\text{LiAlH}_4$  sample was subjected to high-pressure ball milling (HPBM) in hydrogen at 97.5 bar for 20 min to facilitate dispersion of the Ti catalyst. A portion of it was then dehydrogenated at 1 bar, resulting in a typical temperature-programmed desorption (TPD) curve (curve a) exhibiting about 7.5 wt % hydrogen below 200 °C and 4.0 wt % below 130 °C. The inset shows that over 4 wt % hydrogen can be produced at 80 °C when the Ti concentration is increased to 4 mol % and that the Ti-doped  $\text{LiAlH}_4$  system is stable during mechanochemical treatment. After 5 h of dehydrogenation at 90 °C to mimic use of the material, only a small amount of hydrogen (about 1 wt %) remained in the 0.5 mol % Ti-doped  $\text{LiAlH}_4$  sample (curve b). This result indicated that the  $\text{LiAlH}_4$  in the sample not only fully decomposed according to eq 1, but also that about 60 mol % of the  $\text{Li}_3\text{AlH}_6$  in eq 2 had decomposed. Next, the sample was subjected to HPBM in

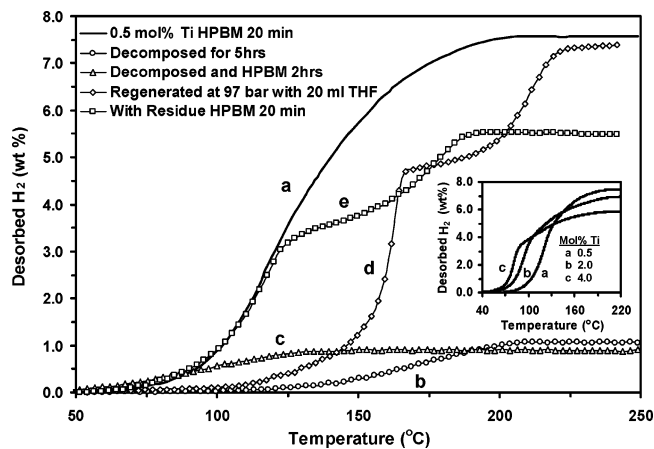


**Figure 2.** Temperature-programmed desorption (TPD) curves (5 °C/min) of 0.5 mol % Ti-doped  $\text{LiAlH}_4$  obtained during one dehydrogenation/rehydrogenation cycle: (a) after high-pressure ball milling (HPBM) in  $\text{H}_2$  at 97.5 bar for 20 min to disperse the Ti catalyst; (b) after dehydrogenation at 90 °C for 5 h to mimic use of the material in an application; (c) after HPBM in  $\text{H}_2$  at 97.5 bar for 2 h after dehydrogenation in a futile attempt to rehydrogenate the sample under dry conditions; (d) after HPBM in  $\text{H}_2$  at 97.5 bar and 20 mL of THF for 2 h to rehydrogenate the sample under wet conditions, followed by filtration and drying, all being key steps in the physiochemical pathway; and (e) after HPBM in  $\text{H}_2$  at 97.5 bar after the residue, obtained from the filtration step and which contains the Ti catalyst and unconverted reactants, was added back to the sample to complete the five-step cycle.

hydrogen at 97.5 bar for 2 h in an attempt to facilitate rehydrogenation. Although the sample proved to be fairly stable with HPBM, and the initial dehydrogenation temperature shifted to a lower temperature from about 100 to about 65 °C, indicating that the dehydrogenation rate of the second reaction could be efficiently improved by HPBM without decomposition, these results proved convincingly that the sample could not be rehydrogenated according to the reverse reactions in eqs 1 and 2 under these conditions. This important and revealing result was in agreement with that reported elsewhere.<sup>12</sup>

Nevertheless, when the HPBM step was carried out not only in hydrogen at 97.5 bar but also in the presence of 20 mL of THF, the  $\text{LiAlH}_4$  was fully rehydrogenated, through the reaction in eq 3 and possibly the reverse reaction in eq 1 (see below). This was the key step in the physiochemical pathway that constituted rehydrogenation of  $\text{LiAlH}_4$ . A fully regenerated sample of  $\text{LiAlH}_4$  was recovered from the THF solution after HPBM, which contained the soluble product  $\text{LiAlH}_4$  and any remaining residue, that is, the insoluble reactants and the catalyst, by simple vacuum filtration to collect the  $\text{LiAlH}_4$  product as a relatively pure precipitate after vacuum-drying at 60 °C to remove any residual THF from the  $\text{LiAlH}_4$ . The catalyst needed to be removed prior to vacuum-drying to prevent dehydrogenation of the sample during this step. Note also that the THF was essentially removed after 6 h of vacuum-drying at 60 °C, because the small amount  $\text{LiCl}$  present in the sample significantly increased the vapor pressure of the THF solution even in the presence of  $\text{LiAlH}_4$ .<sup>15</sup>

A typical TPD curve of a fully regenerated sample of  $\text{LiAlH}_4$  is represented by curve d in Figure 2. It exhibited two characteristic plateau regions corresponding to the reactions in eqs 1 and 2, which respectively released about 4.7 and 2.6 wt % hydrogen, with about 7.3 wt % total hydrogen being released

(15) Del Giudice, F. P. U.S. Patent No. 3453089, 1969.

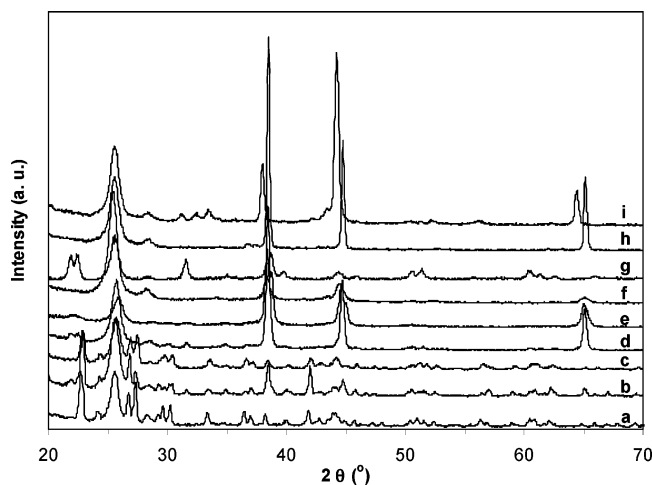


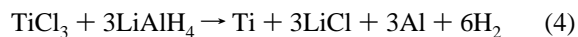
**Figure 3.** XRD patterns of 0.5 mol % Ti-doped LiAlH<sub>4</sub> during one dehydrogenation/rehydrogenation cycle corresponding to the results in Figure 2 and reference materials, showing the structural changes that occurred during various cycle steps and proving conclusively that LiAlH<sub>4</sub> was rehydrogenated according to the five-step physiochemical pathway: (a) purified LiAlH<sub>4</sub> from Et<sub>2</sub>O; (b) rehydrogenated LiAlH<sub>4</sub>; (c) 0.5 mol % Ti-doped LiAlH<sub>4</sub> ball-milled for 20 min in 97.5 bar of H<sub>2</sub>; (d) sample (c) decomposed at 90 °C for 5 h; (e) sample (d) ball-milled for 2 h in 97.5 bar of H<sub>2</sub>; (f) residue obtained from the filter paper after vacuum filtration of the regenerated sample; (g) Li<sub>3</sub>AlH<sub>6</sub> prepared mechanochemically from 2LiH+LiAlH<sub>4</sub> according to a procedure given elsewhere;<sup>16</sup> (h) Al as received; and (i) LiH as received.

after regeneration. Because the Ti catalyst was essentially removed during the filtration step, the dehydrogenation rate was similar to that of an uncatalyzed sample.<sup>12</sup> By adding the residue obtained from the filtration step (which contained the catalyst) back into the regenerated sample and carrying out a HPBM step in hydrogen at 97.5 bar for 20 min (curve e), the dehydrogenation kinetics became very similar to that of the initial sample of Ti-doped LiAlH<sub>4</sub>. The apparent loss in hydrogen capacity was most likely due to some of the LiAlH<sub>4</sub> reacting with any unconverted LiH remaining in the residue to form Li<sub>3</sub>AlH<sub>6</sub>,<sup>16</sup> and perhaps due to some LiAlH<sub>4</sub> decomposing during and because of this final HPBM step.

Overall, the TPD curves in Figure 2 illustrate the key steps that constitute a unique and relatively simple physiochemical pathway for the rehydrogenation of LiAlH<sub>4</sub> from LiH and Al. What remains to be reported here is the systematic verification that proves LiAlH<sub>4</sub> can be rehydrogenated from its decomposition products, along with the effects of a few key parameters, the amount of THF and the hydrogen pressure, on the rehydrogenation kinetics in terms of the conversion of LiAlH<sub>4</sub>. The explanation of the underlying mechanism associated with the key step in the reversible process, that is, the HPBM step carried out in the presence of THF and hydrogen, is also provided.

**Analysis and Verification.** To verify the phase and structural changes that occurred during the dehydrogenation/rehydrogenation cycle of Ti-doped LiAlH<sub>4</sub>, and hence to provide evidence of the rehydrogenation of LiAlH<sub>4</sub> through the physiochemical pathway, X-ray diffraction (XRD) measurements were carried out; the results are presented in Figure 3. After HPBM with Ti, the LiAlH<sub>4</sub> structure remained essentially intact, with no noticeable Li<sub>3</sub>AlH<sub>6</sub> species present in the XRD pattern

(compare curve c with curve a in Figure 3). This result was consistent with the TPD results, again indicating that the LiAlH<sub>4</sub> was stable during mechanochemical treatment. On the other hand, HPBM of the sample caused most of the peaks to become broader, possibly indicating the formation of a fine grain size LiAlH<sub>4</sub>, which may have improved the dispersion of the Ti catalyst during HPBM, as reported elsewhere.<sup>11,12</sup> Also during HPBM, the Ti catalyst necessarily reacted with LiAlH<sub>4</sub> according to the following reaction:<sup>17,18</sup>



perhaps to form the active catalyst species as nanocrystalline sized Ti or TiAl<sub>x</sub> alloy.<sup>18,19</sup> The absence of Al and LiCl phases in the XRD pattern of curve c was probably due to them being present only in very small amounts.

Besides Li<sub>3</sub>AlH<sub>6</sub>, the major species present in the XRD pattern of the decomposed sample were LiH and Al, with no noticeable LiAlH<sub>4</sub> present (curve d). This result was consistent with the TPD results (Figure 2), indicating that the first reaction in eq 1 went to completion and that the second reaction in eq 2 only partially occurred, as previously indicated. The absence of crystalline LiH during the dehydrogenation reactions, as reported elsewhere,<sup>17</sup> might have been due to two reasons. First, the LiH phase overlapped the crystalline Al phase, because the characteristic peaks of these two species were very close to each other; and, second, an amorphous LiH phase might have formed, especially because it has been reported that an amorphous NaH phase forms during the dehydrogenation of Ti-doped NaAlH<sub>4</sub>.<sup>19</sup>

After 2 h of HPBM, in an attempt to rehydrogenate the sample without THF, the only species detected were Li<sub>3</sub>AlH<sub>6</sub> and Al, indicating no reversibility of the reaction in eq 1 under these somewhat drastic conditions (curve e). The observed peak broadening (compare curve e with curve d in Figure 3) was again consistent with the formation of a fine grain size Li<sub>3</sub>AlH<sub>6</sub>, possibly with a better dispersed catalyst, which might explain the improvement in the dehydrogenation rate of Li<sub>3</sub>AlH<sub>6</sub> (compare curve c with curve b in Figure 2). The XRD pattern of the rehydrogenated LiAlH<sub>4</sub> sample (curve b) obtained from the filtrate after vacuum-drying matched very well with the XRD pattern associated with the pure LiAlH<sub>4</sub> (curve a), with only small amounts of Li<sub>3</sub>AlH<sub>6</sub> and Al being present. Li<sub>3</sub>AlH<sub>6</sub> and Al probably formed from the partial dehydrogenation of LiAlH<sub>4</sub> during the vacuum-drying step, because Li<sub>3</sub>AlH<sub>6</sub> is insoluble in THF, and it was unlikely that Li<sub>3</sub>AlH<sub>6</sub> and Al passed through the filter paper.

In contrast, only the Al phase appeared in the XRD pattern of the residue sample (curve f). The absence of LiH and Ti phases was probably due to the formation of nanosized crystalline or amorphous particles.<sup>19</sup> These results suggested that probably most of the LiH reacted according to eq 3 instead of sequentially following the reverse reactions in eq 2 followed by eq 1, and perhaps that all of the Li<sub>3</sub>AlH<sub>6</sub> was regenerated back to LiAlH<sub>4</sub> through the reverse reaction in eq 1, because Li<sub>3</sub>AlH<sub>6</sub> is insoluble in THF and because no Li<sub>3</sub>AlH<sub>6</sub> phase was

(16) Zaluska, A.; Zaluski, L.; Ström-Olsen, J. O. *J. Alloys Compd.* **1999**, *290*, 71–78.

(17) Easton, D. S.; Schneibel, J. H.; Speakman, S. A. *J. Alloys Compd.* **2005**, *398*, 245–248.

(18) Balema, V.; Wiench, J. W.; Dennis, K.; Pruski, M.; Pecharsky, V. *J. Alloys Compd.* **2001**, *329*, 108–114.

(19) Felderhoff, M.; Klementiev, K.; Grunert, W.; Spliethoff, B.; Tesche, B.; Bellosta von Colbe, J. M.; Bogdanoviv, B.; Hartel, M.; Pommerin, A.; Schuth, F.; Weidenthaler, C. *Phys. Chem. Chem. Phys.* **2004**, *6*, 4369–4374.



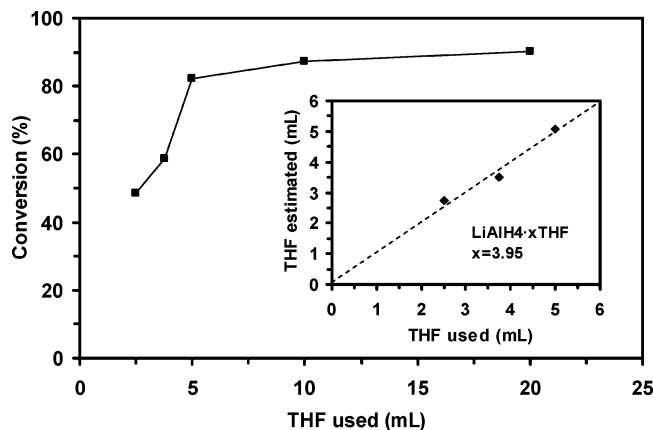


**Figure 4.** Effect of the amount of THF used on the rehydrogenation kinetics of  $\text{LiAlH}_4$  in terms of conversion of  $\text{LiAlH}_4$ . All of these experiments were carried out using the same procedure as described in Materials and Methods with the rehydrogenation pressure at 97.5 bar. The inset shows a linear correlation between the amount of THF used and that predicted, which was obtained from knowing the amount of regenerated  $\text{LiAlH}_4$  in the THF solution and by varying  $x$  in the complex formula  $\text{LiAlH}_4 \cdot x\text{THF}$  until the data aligned with the diagonal. The results in the inset verified not only that the conversion was limited by the amount of THF, but also that the  $\text{LiAlH}_4 \cdot 4\text{THF}$  adduct formed, in agreement with that reported in the literature.<sup>20</sup>

present in the residue sample (curve f). Clearly, all of the  $\text{Li}_3\text{AlH}_6$  in the decomposed sample (see curves b and c in Figure 2) necessarily produced  $\text{LiAlH}_4$  through the reverse reaction of eq 1.

It is noteworthy that these experimental results are in agreement with those reported elsewhere<sup>13,14</sup> and discussed in the Introduction. For example, no reaction occurred in the absence of THF; nor did any reaction take place in  $\text{Et}_2\text{O}$  under the same conditions used with THF (i.e., ambient temperature and up to 100 bar of hydrogen). These results also suggested that the THF played the critical role in fostering the rehydrogenation of  $\text{LiAlH}_4$ , through the key step in the physiochemical pathway, that is, the HPBM step in the presence of both THF and hydrogen.

The effect of the amount of THF on the rehydrogenation kinetics in terms of the conversion of  $\text{LiAlH}_4$  is displayed in Figure 4. The conversion increased with an increase in the THF to just over 90% when 20 mL of THF was used. It then dropped, but only by about 10% down to 80% or so, even when as little as 5 mL of THF was used. However, the conversion dropped much more quickly down to about 50% and nearly linearly with the THF decreasing from 5 to 2.5 mL. These results show that very high conversions can be obtained with THF at ambient temperature and a reasonable but somewhat high pressure. Recall that, in the absence of THF, the conversion was zero at these conditions (Figure 2, curve b). It is shown below that much lower pressures can also be used.

The inset shows a linear correlation between the amount of THF used and that predicted, which was obtained from knowing the amount of regenerated  $\text{LiAlH}_4$  in the THF solution and by varying  $x$  in the adduct formula  $\text{LiAlH}_4 \cdot x\text{THF}$  until the data aligned with the diagonal. This correlation not only verified that the conversion was limited by the amount of THF, but also that the  $\text{LiAlH}_4 \cdot 4\text{THF}$  adduct formed between  $\text{LiAlH}_4$  and THF,<sup>20</sup>

which explained why the curve in Figure 4 decreased significantly when small amounts of THF were used. An understanding of this behavior was obtained from the properties of  $\text{LiAlH}_4$  in ethereal solutions.

The physical and chemical properties of  $\text{LiAlH}_4$  in ethereal solutions have been investigated by conductometric, ebullioscopic, and spectroscopic techniques.<sup>20–22</sup> These studies showed that the ion pairs of  $\text{LiAlH}_4$  in THF are solvent separated and exist in two concentration-dependent equilibria: an equilibrium between ion pairs and free ions at low concentration ( $<0.1$  M THF), and the formation of triple ions at higher concentrations ( $\sim 0.4$  M THF). In contrast,  $\text{LiAlH}_4$  in diethyl ether was reported to be concentration-independent and form only contact ions,<sup>20,21</sup> which might explain the lack of rehydrogenation of  $\text{LiAlH}_4$  in  $\text{Et}_2\text{O}$ . Moreover, the NMR results showed that the  $\text{LiAlH}_4$  is solvated by four molecules of THF, thereby indicating the formation of a  $\text{LiAlH}_4 \cdot 4\text{THF}$  adduct.<sup>20</sup> Infrared and Raman results suggested that the trend in the ordering of the cation solvation goes as:  $\text{Li}-\text{Et}_2\text{O} \ll \text{Li}-\text{THF} < \text{Li}-\text{diglyme}$ , and that THF strongly attaches to  $\text{Li}^+$  in  $\text{LiAlH}_4$ , forming a four-coordinated lithium solvate.<sup>20,22</sup> Moreover, the change in the formation enthalpy of  $\text{LiAlH}_4$  as solvent separated ion pairs in THF was estimated to be  $-32$  kJ/mol lower than that associated with  $\text{LiAlH}_4$  as contact ion pairs in  $\text{Et}_2\text{O}$ , in the temperature range from  $-70$  to  $25$  °C.<sup>20,23,24</sup> Also, the ion aggregation of  $\text{LiAlH}_4$  in THF from lower to higher concentrations was estimated to be exothermic.<sup>22</sup> Therefore, it was surmised that  $\text{LiAlH}_4$  was more stable in THF than in  $\text{Et}_2\text{O}$  due to a  $-30$  to  $-40$  kJ/mol enthalpy change.

Furthermore, the value of the standard free energy of the reaction in eq 3, that is, the formation of  $\text{LiAlH}_4$  from  $\text{LiH}$  and  $\text{Al}$ , ranges from 21.7 kJ/mol<sup>25</sup> to 34.27 kJ/mol;<sup>26</sup> and that associated with the reverse reaction in eq 1, that is, the formation of  $\text{LiAlH}_4$  from  $\text{Li}_3\text{AlH}_6$  and  $\text{Al}$ , ranges from 18.7 kJ/mol<sup>25</sup> to 27.68 kJ/mol.<sup>26</sup> Therefore, these reactions do not occur spontaneously. To make these reactions more thermodynamically favorable, the enthalpies and or entropies of these reactions must change. Although the entropies can be changed by increasing the hydrogen pressure, it requires a very high pressure to make the reaction in eq 3 thermodynamically favorable; and for the reverse reaction in eq 1, it requires at least 1000 bar.<sup>27</sup> On the other hand, if the enthalpies of these reactions can become more exothermic, they may become thermodynamically favored. Based on the results of this study, it was surmised that this did in fact occur, as a result of the solvation effect associated with  $\text{LiAlH}_4$  forming solvent separated ion pairs in THF. With no  $\text{LiAlH}_4$  regeneration occurring even at hydrogen pressures up to 100 bar, with no regeneration occurring in diethyl ether, and with the conversion of these reactions limited by the formation of a  $\text{LiAlH}_4 \cdot 4\text{THF}$  adduct, all of these results suggested that the enthalpy change associated with the solvation of THF with  $\text{LiAlH}_4$  to form the  $\text{LiAlH}_4 \cdot 4\text{THF}$  adduct made these reactions

(21) Ashby, E. C.; Dobbs, F. R.; Hopkins, H. P. *J. Am. Chem. Soc.* **1975**, *97*, 3158–3162.

(22) Shirk, A. E.; Shriver, D. F. *J. Am. Chem. Soc.* **1973**, *95*, 5904–5912.

(23) Hogen-Esch, T. E.; Smid, J. *J. Am. Chem. Soc.* **1966**, *88*, 307–318.

(24) Hogen-Esch, T. E.; Smid, J. *J. Am. Chem. Soc.* **1966**, *88*, 318–324.

(25) Chase, M. W., Jr. *NIST-JANAF Thermochemical Tables*, ed. 4 (*J. Phys. Chem. Ref. Data, Monograph*, **1998**, *9*, 1–1951) (NIST Webbook: <http://webbook.nist.gov/cgi/cbook.cgi?Source=1998CHA1-1951&Units=SI&Mask=2>).

(26) Dymova, T. N.; Aleksandrov, D. P.; Konoplev, V. N.; Silina, T. A.; Sizareva, V. S. *Russ. J. Coord. Chem.* **1994**, *20*, 263–268.

(27) Jang, J.; Shim, J.; Cho, Y. W.; Lee B. *J. Alloys Compd.* **2006**, in press.

(20) Ashby, E. C.; Dobbs, R. R.; Hopkins, H. P. *J. Am. Chem. Soc.* **1973**, *95*, 2823–2829.

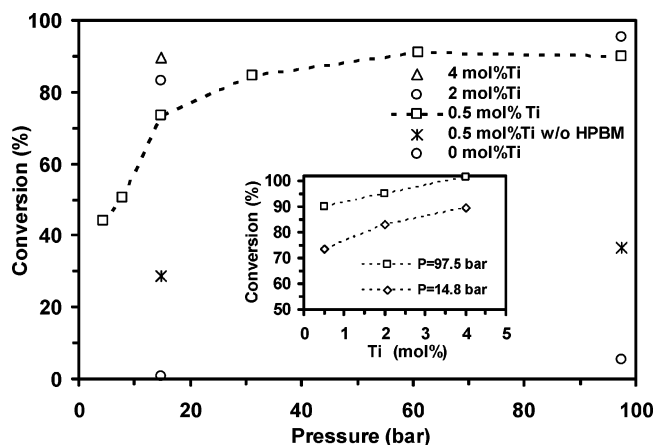


**Figure 5.** Effect of the H<sub>2</sub> pressure on the rehydrogenation kinetics of LiAlH<sub>4</sub> in terms of conversion of LiAlH<sub>4</sub>, along with the effects of the Ti catalyst concentration, and high-pressure ball milling (HPBM). All of these experiments were carried out using the same procedure as described in Materials and Methods with the volume of THF fixed at 20 mL. The effect of the Ti catalyst concentration on conversion is shown more concisely in the inset.

thermodynamically favorable and hence easily reversible by the physiochemical pathway.

Finally, the effect of the hydrogen pressure on the hydrogenation kinetics of LiAlH<sub>4</sub> in terms of the conversion of LiAlH<sub>4</sub> is shown in Figure 5, along with the effects of the Ti catalyst concentration and HPBM. In the 60–98 bar range of hydrogen pressures, the conversion remained almost constant and quite high at about 90%, whereas it dropped to about 73% at 14.8 bar. Even at very low hydrogen pressures, the reaction still exhibited considerable hydrogenation kinetics, as gleaned from the conversion being 44% at 4.5 bar. It must be emphasized that the pressure in the closed vessel after the HPBM regeneration step was always substantially lower than the initial pressure due to rehydrogenation. In fact, it was estimated that the reaction might occur with reasonable kinetics even at hydrogen pressures as low as 1 bar.

With respect to the catalyst concentration, the results in Figure 5 show that, although it was possible to regenerate LiAlH<sub>4</sub> without Ti present, the kinetics were extremely slow. Less than 1% conversion was achieved at 14.8 bar and only about 5% at 97.5 bar. In contrast, the sample doped with as little as 0.5 mol % Ti exhibited excellent kinetics, with conversions of 73% and 90% at 14.8 and 97.5 bar, respectively. The inset shows that when the Ti catalyst concentration was increased from 0.5 to 4 mol %, the conversion increased almost linearly from 73% to 90% at low pressure (14.8 bar) and from 90% to 100% at high pressure (97.5 bar). Clearly, the hydrogenation kinetics of LiAlH<sub>4</sub> formation improved markedly in the presence of a small amount of the Ti catalyst. The mechanistic role of Ti is not understood; nor is it understood for the well-studied Ti-doped NaAlH<sub>4</sub> system.<sup>8</sup> Nevertheless, it is clear from these results and those presented in Figure 2 that the Ti catalyst is ineffective in the absence of THF, suggesting that the Ti is in some way acting on the LiAlH<sub>4</sub>·4THF adduct.

With respect to HPBM, the results in Figure 5 show that even without a HPBM step, a conversion of around 30% was obtained for the 0.5 mol % Ti-doped LiAlH<sub>4</sub> sample. However, the conversion was always less than one-half that obtained with HPBM. This result further substantiated that the HPBM step,

when combined with THF, significantly improved the hydrogenation kinetics. Plausible reasons include HPBM increasing the collisions between the solid, liquid, and gas reactants, or providing extra thermal energy (converted from mechanical energy) that facilitated the reaction.<sup>28</sup>

## Conclusions

A novel physiochemical pathway for the cyclic dehydrogenation and rehydrogenation of LiAlH<sub>4</sub> from Li<sub>3</sub>AlH<sub>6</sub>, LiH, and Al was clearly illuminated. The notion of using a liquid complexing agent, such as THF, in conjunction with a Ti catalyst and a hydrogen atmosphere during high-pressure ball milling, to promote reversibility of the hydrogenation reactions that form LiAlH<sub>4</sub>·4THF adduct in THF was found to play the essential role in fostering rehydrogenation. The Ti-doped LiAlH<sub>4</sub> produced by this physiochemical pathway exhibited a hydrogen storage capacity of around 4 wt % in the 100 °C range, making it perhaps one of the best performing hydrogen storage materials known. It was also easily rehydrogenated simply by using THF and the physiochemical route at essentially ambient temperature and pressures of 4.5–97.5 bar, with the THF being fully recoverable.

Overall, this cyclic process could make LiAlH<sub>4</sub> one of the more attractive materials for stationary hydrogen storage applications. However, this novel methodology needs to be further explored with other higher capacity hydrogen storage materials, most likely, but not exclusively, belonging to the metal complex hydride class of materials, especially to meet the more stringent requirements for transportation applications. Additional mechanistic understanding of the key steps in this physiochemical pathway is also needed to foster the development of useful hydrogen storage materials for commercial applications through this approach.

## Materials and Methods

TiCl<sub>3</sub> (Aldrich, 99.99%, anhydrous), aluminum powder (Alfa Aesar, 99.97%), and LiH (Aldrich, 95%) were used as received. LiAlH<sub>4</sub> powder (Aldrich, 95%) was recrystallized from a 3 M diethyl ether (Et<sub>2</sub>O) (Aldrich, 99.9%, anhydrous) solution, filtered through 0.7 μm filter paper, and vacuum-dried. The typical procedure associated with carrying out one dehydrogenation/rehydrogenation cycle with LiAlH<sub>4</sub> proceeded as follows. 1 g of LiAlH<sub>4</sub> was mixed with the catalyst precursor (TiCl<sub>3</sub>) to produce a doped sample containing up to 4 mol % metal relative to Na. The sample was then ball-milled for 20 min at different hydrogen pressures (National Welders, UHP, 99.995%) ranging from 4.5 to 97.5 bar using a SPEX 8000 high-energy ball mill loaded with a 65 cm<sup>3</sup> SS vial containing a single SS ball (8.2 g) with a diameter of 1.3 cm. After being ball-milled, the sample was subjected to dehydrogenation by heating at 90 °C for 5 h. The dehydrogenated sample was then ball-milled for 2 h at different hydrogen pressures ranging from 4.5 to 97.5 bar. Afterward, tetrahydrofuran (THF) (Aldrich, 99.9%, anhydrous) ranging from 2.5 to 20 mL was added to this sample, and the mixture was ball-milled for an additional 2 h at different hydrogen pressures ranging from 4.5 to 97.5 bar. The resulting heterogeneous mixture containing both soluble and insoluble compounds was vacuum filtered through 0.7 μm filter paper and vacuum-dried to collect the rehydrogenated LiAlH<sub>4</sub> from the dehydrogenated material as a precipitate from the filtrate. The residue remaining on the filter paper, consisting of insoluble reactants and catalyst, was collected and

(28) Wang, G. W.; Komatsu, K.; Murata, Y.; Shiro, M. *Nature* **1997**, *387*, 583–586.

used to redope the sample with catalyst as the final step in the physiochemical pathway. All sample handling procedures were performed in a nitrogen glovebox. The conversion was calculated on the basis of the amount of sample obtained from the filtrate after rehydrogenation divided by the total amount of sample collected after the rehydrogenation step, including the filtrate plus the residue on the filter paper.

Thermogravimetric analysis was carried out with a Perkin-Elmer TGA 7 Series thermogravimetric analyzer (TGA). The dehydrogenation rates of various doped and ball-milled samples of  $\text{LiAlH}_4$  were measured at atmospheric pressure in helium (National Welders, UHP, 99.995%) flowing at  $\sim 60 \text{ cm}^3/\text{min}$  in a temperature-programmed desorption (TPD) mode. For TPD runs, the samples were heated to  $250 \text{ }^\circ\text{C}$  at a

ramping rate of  $5 \text{ }^\circ\text{C}/\text{min}$  after purging with helium for 1 min. Approximately 10 mg of sample was used in each TPD run.

The structural/compositional changes of the samples were identified through X-ray diffraction (XRD) measurements using a Rigaku D-max B single axis diffractometer with a  $\text{Cu K}\alpha$  ( $\lambda = 0.1543 \text{ nm}$ ) radiation source. The sample was protected by a piece of cellophane film to avoid exposure to moisture and oxygen. The peaks at  $2\theta = 25.5$  and  $28.6$  were due to the diffraction caused by the film.

**Acknowledgment.** Financial support provided by the DOE through Cooperative Agreement DE-FC36-04GO14232 is greatly appreciated.

JA060045L